

Finite Temperature Excitations of an anisotropically trapped Bose gas : A diffusion Monte Carlo study

S. Datta

S. N. Bose National Centre for Basic Sciences

February 8, 2020

Abstract

We calculate the excitation frequencies of $m=0$ mode and $m=2$ mode of Rb^{87} atoms confined in an anisotropic trap and interacting with repulsive forces by diffusion Monte Carlo method. The spectrum turns out to be strongly temperature dependent and we compare our results with other theories and experiments. This is the first Monte Carlo calculation for a trapped Bose Einstein condensed dilute gas which shows an excellent agreement with the JILA data for $m=2$ mode all the way up to $T = 0.9T_c$ whereas most of the previous mean field type calculations had shown agreement with the experimental data only up to $T = 0.6T_c$.

1 Introduction

After the experimental realization of Bose Einstein Condensation in alkali vapors in 1995[1], and subsequent experiments pertinent to temperature dependence of frequencies and damping rate[2], there have been a lot of theoretical studies [3-6] to explain the experimental observations in connection with temperature dependent frequency shifts corresponding to different angular momenta, $m=0$ and $m=2$ modes in particular[2]. Results have been reported in which theoretical data agreed well with experimental values for $m=0$ mode showing an upward trend of frequencies with rise in temperature [4,6]. But in all cases the agreement is rather poor when it comes to $m=2$ mode. There is an agreement up to $T = 0.6T_c$, beyond which frequencies rise with increase in temperature deviating from the downward trend of experimental data. In this article, we would like to report a diffusion Monte Carlo study of the frequency shifts of $m=2$ and $m=0$ modes in a dilute gas of Rb^{87} . In our non mean field study, we see agreement with experimental study for $m=2$ mode all the way to $T = 0.9T_c$ [Fig. 10]. On the other hand our $m=0$ calcualtion agrees with previous gapless theory[5] showing the same downward shift of the frequencies the critical temperature is approached.

The dynamical behavior of dilute alkali BECs at $T=0$ can be well described by Gross-Pitaevski eqn(GPE)[7].

$$i\hbar \frac{\partial \phi(\vec{r}, t)}{\partial t} = \left[-\frac{\hbar^2}{2m} \frac{\Delta}{2} + V_{ext}(\vec{r}) + g|\phi(\vec{r}, t)|^2 \right] \phi(\vec{r}, t) \quad (1)$$

where $g = \frac{4\pi\hbar^2 a}{m}$.

But it seems to be inadequate at finite temperatures. The other mean field theories which have been used so far, are based on HF and HFB-Popov equations [8] and break down near T_c as its effective single particle spectrum always displays a gap. In 1998, a self consistent gapless non-divergent theory was[5] developed and a closed set of coupled equations were solved numerically. Analytic expressions[6] for temperature dependent frequencies were obtained for $m=0$ and $m=2$ by extending the time dependent variational

technique from zero to finite temperatures as follows :

$$\omega(|m|=2) = \omega\sqrt{2[1 - f_3(T)]} \quad (2)$$

$$\omega(|m|=0) = \omega\sqrt{\frac{1 - f_3(T)}{2}}[4 + 3\lambda^2(T) \pm \sqrt{16 + 9\lambda^4(T) - 16\lambda^2(T)}] \quad (3)$$

The total density of the atoms is related to BEC density and normal component as follows: At T=0 the normal component is not equal to zero in the interacting case and is referred to as 'quantum depletion'. At finite temperature, thermal atoms also contribute to the normal component. Since mean field wavefunctions do not account for the normal component, it gives accurate energy spectrum if depletion is small[9]. Near T_c , the quantum depletion becomes significant and mean field treatment breaks down. Eventhough Ref[5] has the best agreement with JILA data till date, solving coupled partial differential equations numerically is not an easy task. The chief purpose of this paper is to go beyond field theory with a comparatively simpler numerical procedure which would work at all temperatures. We propose to explore finite temperature aspect of BEC by quantum non-perturbative technique, namely Generalized Feynman- Kac (GFK)[10] procedure. Since Quantum Monte Carlo methods are expensive, we are simulating only 100 interacting atoms at this moment.

The paper is organized as follows : In Sec II we discuss the path integral technique at zero and finite temperature as a many body technique, the Schroedinger formulation of Rb condensate, fundamental concepts of BEC and finite temperature excitations. In Sec III we discuss the numerical procedure. In Sec IV we present all the numerical results pertinent to energies and frequencies at different temperature. Finally in Sec V we summarize our achievements.

2 Theory

To connect Generalized Feynman Kac (GFK) to other many body techniques our numerical procedure (GFK)[11-12] has a straightforward implementation to Schroedinger's wave mechanics . Since at low temperature the de Broglie wavelength of the atoms become appreciable, we do full quantum treatment. GFK is essentially a path integral technique with trial functions for which operations of the group of the wave function keep points in the chosen nodal region, provide an upper bound for the lowest state energy of that symmetry. The nodal region with the lowest energy serves as a least upper bound. If the nodal region has exact nodal structures of the true wave function the random walk is exact in the limit scale, time for walk, and number of walks get arbitrarily large. To calculate energy we approximate an exact solution (i.e., the GFK representation of it) to the Schroedinger's equation, whereas most of the other numerical procedures approximate a solution to an approximate Schroedinger equation. From the equivalence of the imaginary time propagator and temperature dependent density matrix, finite temperature results can be obtained from the same zero temperature code by running it for finite time. So from all these aspects, Generalised Feynman-Kac method turns out to be a potentially good candidate as a sampling procedure for Bose gases at all temperatures.

2.1 Path integral Theory at T=0

For the Hamiltonian $H = -\Delta/2 + V(x)$ consider the initial value problem

$$\begin{aligned} i\frac{\partial u}{\partial t} &= \left(-\frac{\Delta}{2} + V\right)u(x, t) \\ u(0, x) &= f(x) \end{aligned} \tag{4}$$

with $x \in R^d$ and $u(0, x) = 1$. The solution of the above equation can be written in Feynman-Kac representation as

$$u(t, x) = E_x \exp\left\{-\int_0^t V(X(s))ds\right\} \tag{5}$$

where $X(t)$ is a Brownian motion trajectory and E is the average value of the exponential term with respect to these trajectories. The lowest energy

eigenvalue for a given symmetry can be obtained from the large deviation principle of Donsker and Varadhan [13],

$$\lambda = - \lim_{t \rightarrow \infty} \frac{1}{t} \ln E_x \exp - \int_0^t V(X(s)) ds \quad (6)$$

In dimensions higher than 2, the trajectory $x(t)$ escapes to infinity with probability 1. As a result, the important regions of the potential are sampled less and less frequently and the above equation converges slowly. To formulate the generalized Feynman-Kac method we first rewrite the Hamiltonian as $H = H_0 + V_p$, where $H_0 = -\Delta/2 + \lambda_T + \Delta\psi_T/2\psi_T$ and $V_p = V - (\lambda_T + \Delta\psi_T/2\psi_T)$. Here ψ_T is a twice differentiable nonnegative reference function and $H\psi_T = \lambda_T\psi_T$. The expression for the energy can now be written as

$$\lambda = \lambda_T - \lim_{t \rightarrow \infty} \frac{1}{t} \ln E_x \exp - \int_0^t V_p(Y(s)) ds \quad (7)$$

where $Y(t)$ is the diffusion process which solves the stochastic differential equation

$$dY(t) = \frac{\Delta\psi_T(Y(t))}{\psi_T(Y(t))} dt + dX(t) \quad (8)$$

The presence of both drift and diffusion terms in this expression enables the trajectory $Y(t)$ to be highly localized. As a result, the important regions of the potential are frequently sampled and Eq (14) converges rapidly.

2.2 Path integral theory at finite temperature

The temperature dependence comes from the realization that the imaginary time propagator is identical to the temperature dependent density matrix if $t \Rightarrow \beta = 1/T$ holds.

This becomes obvious when we consider the eqs[14]

$$-\frac{\partial k(2, 1)}{\partial t_2} = H_2 k(2, 1) \quad (9)$$

and

$$-\frac{\partial \rho}{\partial \beta} = H_2 \rho(2, 1) \quad (10)$$

and compare

$$k(2, 1) = \sum_i \phi_i(x_2) \phi_i^*(x_1) e^{-(t_2 - t_1) E_i} \quad (11)$$

and

$$\rho(2, 1) = \sum_i \phi_i(x_2) \phi_i^*(x_1) e^{-\beta E_i} \quad (12)$$

For Zero temp FK we had to extrapolate to $t \Rightarrow \infty$. For finite run time t in the simulation, we have finite temparature results. In this section we show how we change our formalism to go from zero to finite temparature. We begin with the definition of finite temparature. A particular temparature 'T' is said to be finite if $\Delta E < kT$ holds. The temperature dependent density matrix can be written in the following form

$$\rho(x, x', \beta) = \rho^{(0)}(x, x', \beta) \times \langle \exp[-\int_0^\beta V_p[X(s)]ds] \rangle_{DRW} \quad (13)$$

The partition function can be recovered from the above as follows:

$$\int \rho(x, x, \beta) dx = \int \rho^{(0)}(x, x, \beta) dx \times \langle \exp[-\int_0^\beta V_p[X(s)]ds] \rangle_{DRW} \quad (14)$$

In the usual notation, the above equation reads as

$$Z(x, \beta) = Z^0(x, \beta) \times \langle \exp[-\int_0^\beta V_p[X(s)]ds] \rangle_{DRW} \quad (15)$$

At finite temperature thus free energy can be written as

$$F = -\ln Z(x, \beta) / \beta = -\ln Z^0(x, \beta) / \beta - \ln \langle \exp[-\int_0^\beta V_p[X(s)]ds] \rangle_{DRW} / \beta \quad (16)$$

2.3 Schroedinger Formalism for Rb condensate

In cylindrical symmetry, m=2 mode is an uncoupled one and there are two coupled oscillations for m=0 mode [15]. We choose to work in the cylindrical coordinates as the original experiment had an axial symmetry, cylindrical coordinates are the natural choices for this problem. We consider a cloud of N atoms interacting through repulsive potential placed in a three dimensional harmonic oscillator potential. At low energy the motion of condensate can be represented as

$$[-\Delta/2 + V_{int} + \frac{1}{2} \sum_{i=1}^N [x_i^2 + y_i^2 + \lambda z_i^2] \psi(\vec{r}) = E\psi(\vec{r}) \quad (17)$$

where $\frac{1}{2} \sum_{i=1}^N [x_i^2 + y_i^2 + \lambda z_i^2] \psi(\vec{r})$ is the anisotropic potential with anisotropy factor $\lambda = \frac{\omega_z}{\omega_x}$. Now

$$V_{int} = V_{Morse} = \sum_{i,j} V(r_{ij}) = \sum_{i < j} D[e^{-\alpha(r-r_0)}(e^{-\alpha(r-r_0)} - 2)] \quad (18)$$

The above Hamiltonian is not separable in spherical polar coordinates because of the anisotropy. In cylindrical coordinates the noninteracting part behaves as a system of noninteracting harmonic oscillators and can be written as follows :

$$\begin{aligned} & [-\frac{1}{2\rho} \frac{\partial}{\partial \rho} (\rho \frac{\partial}{\partial \rho}) - \frac{1}{\rho^2} \frac{\partial^2}{\partial \phi^2} - \frac{1}{2} \frac{\partial^2}{\partial z^2} \\ & + \frac{1}{2} (\rho^2 + \lambda^2 z^2)] \psi(\rho, z) \\ & = E\psi(\rho, z) \end{aligned} \quad (19)$$

The energy 'E' of the above equation can be calculated exactly which is

$$E_{n_\rho n_z m} = (2n_\rho + |m| + 1) + (n_z + 1/2)\lambda \quad (20)$$

In our guided random walk we use the noninteracting solution of Schoroedinger equation as the trial function as follows [16]:

$$\psi_{n_\rho n_z m}(r) \simeq \exp^{\frac{-z^2}{2}} H_{n_z}(z) \times e^{im\phi} \rho^m e^{-\rho^2/2} L_{n_\rho}^m(-\rho^2) \quad (21)$$

2.4 Fundamentals of BEC

Even though the phase of Rb vapors at $T=0$ is certainly solid, Bose condensates are preferred in the gasous form over the liquids and solids because at those higher densities interactions are complicated and hard to deal with on an elementary level. They are kept metastable by maintaining a very low density. For alkali metals, η , the ratio of zero point energy and molecular binding energy lies between 10^{-5} and 10^{-3} . According to the theory of corresponding states[17] since for the $T=0$ state of alkali metals, η exceeds a critical value 0.46, the molecular binding energy dominates over the zero point motion and they condense to solid phase. But again the life time of a gas is limited by three body recombination rate which is proportional to the square of the atomic density. It gets suppressed at low density. Magnetically trapped alkali vapors can be metastable depending on their densities and lifetimes. So keeping the density low only two body collisions are allowed as a result of which dilute gas approximation [18] still holds for condensates which tantamounts to saying $na^3 \ll 1$ (a is the scattering length of s wave). Now defining $n = N/V = r_{av}^{-3}$ as a mean distance between the atoms (definition valid for any temperature), the dilute gas condition reads as $a \ll r_{av}$ and zero point energy dominates (dilute limit). In the dense limit, for $a \approx r_{av}$ on the other hand the interatomic potential dominates. The gas phase is accomplished by reducing the material density through evaporative cooling.

2.5 Finite temperature Excitations :

Finite temperature excitation spectrum is obtained by using the path integral formalism used in Section 2.2. In our analysis, we assume that the condensate oscillates in a static thermal cloud. There are no interactions between the condensate and the thermal cloud. The principal effect of finite temperature on the excitations is the depletion of condensate atoms. We want to calculate the collective excitations of Bose Einstein condensates corresponding to JILA Top experiment ($m=2$ and $m=0$ mode).

Condensation fraction and Critical temperature : In the noninteracting case for a harmonic type external force the theoretical prediction for condensation fraction is

$$N_0/N = 1 - (T/T_c)^3 \quad (22)$$

Critical temperature can be defined as

$$T_c = \frac{0.94 \times \hbar \bar{\omega} N^{1/3}}{k_B} \quad (23)$$

$$\bar{\omega} = (\omega_\rho^2 \omega_z)^{1/3} \quad (24)$$

From Eq.(22), we see that as temperature increases, condensation fraction decreases in the noninteracting case. Interaction lowers the condensation fraction for repulsive potentials. Some particles always leave the trap because of the repulsive nature of the potential and on the top of it, if temperature is increased further, more particles will fall out of the trap and get thermally distributed. This decrease in condensation fraction eventually would cause the shifts in the critical temperature. We would observe this in Section 4.2 (Fig. 8). Earlier this was done by W. Krauth[19] for a large number of atoms by path integral Monte Carlo method.

3 Numerical procedure

3.1 Dilute limit

In the dilute limit and at very low energy only binary collisions are possible and no three body recombination is allowed. In such two body scattering at low energy first order Born approximation is applicable and the interaction strength 'D' can be related to the single tunable parameter of this problem, the s-wave scattering length 'a' through the relation given below. This single parameter can specify the interaction completely without the detail of the potential in the case of pseudopotentials. We use Morse potential because it has a more realistic feature of having repulsive core at $r_{ij} = 0$ than other model potentials. In our case the interaction strength depends on two more additional parameters, r_0 and α .

$$a = \frac{mD}{4\pi\hbar^2} \int V(r)d^3r \quad (25)$$

The Morse potential for dimer of rubidium can be defined as

$$\sum_{i,j} V(r_{ij}) = \sum_{i < j} D[e^{-\alpha(r-r_0)}(e^{-\alpha(r-r_0)} - 2)] \quad (26)$$

Using the above potential

$$D = \frac{4\hbar^2 a \alpha^3}{m e^{\alpha r_0} (e^{\alpha r_0} - 16)} \quad (27)$$

The Hamiltonian for Rb gas with an asymmetric trapping potential and Morse type mutual interaction can be written as

$$\begin{aligned} & [-\hbar^2/2m \sum_{i=1}^N \nabla_i'^2 + \sum_{i,j} V(r_{ij}')] \\ & + \frac{m}{2} (\omega_x^2 \sum_{i=1}^N x_i'^2 + \omega_y^2 \sum_{i=1}^N y_i'^2 + \omega_z^2 \sum_{i=1}^N z_i'^2)] \psi(\vec{r}') \\ & = E \psi(\vec{r}') \end{aligned} \quad (28)$$

The above Hamiltonian can be rescaled by substituting $\vec{r}' = s\vec{r}$ and $E = E_0 U$ as

$$[-\frac{\hbar^2}{2ms^2} \sum_{i=1}^N \nabla_i'^2 + \sum_{i < j} \frac{4\hbar^2 a \alpha^3}{ms^3 e^{\alpha r_0} (e^{\alpha r_0} - 16)} [e^{-\alpha(r_{ij}' - r_0)} (e^{-\alpha(r_{ij}' - r_0)} - 2)]]$$

$$\begin{aligned}
& + \frac{ms^2}{2} (\omega_x^2 \sum_{i=1}^N x_i^2 + \omega_y^2 \sum_{i=1}^N y_i^2 + \omega_z^2 \sum_{i=1}^N z_i^2) \psi(\vec{r}) \\
= & \quad E_0 U \psi(\vec{r}) \tag{29}
\end{aligned}$$

$$\begin{aligned}
& \left[\frac{1}{2} \sum_{i=1}^N \nabla_i^2 - 4 \frac{a\alpha^3}{se^{\alpha r_0} (e^{\alpha r_0} - 16)} \sum_{i < j} [e^{-\alpha(r_{ij} - r_0)} (e^{-\alpha(r_{ij} - r_0)} - 2)] \right. \\
& \left. - \frac{m^2 \omega_x^2 s^4}{2\hbar^2} \sum_{i=1}^N (x_i^2 + \frac{\omega_y^2}{\omega_x^2} y_i^2 + \frac{\omega_z^2}{\omega_x^2} z_i^2) \right] \psi(\vec{r}) \\
= & \quad -E_0 \frac{Ums^2}{\hbar^2} \psi(\vec{r}) \tag{30}
\end{aligned}$$

Let $\frac{m^2 \omega_x^2 s^4}{\hbar^2} = 1 \Rightarrow s^2 = \frac{\hbar}{m\omega_x}$ is the natural unit of length. Let $\frac{Ums^2}{\hbar^2} = 1 \Rightarrow U = \frac{\hbar^2}{ms^2} = \hbar\omega_x$ is the natural unit of energy. Then the standard form of the equation becomes

$$\begin{aligned}
& \left[\frac{1}{2} \sum_{i=1}^N \nabla_i^2 - \sum_{i < j} 4 \frac{a\alpha^3}{se^{\alpha r_0} (e^{\alpha r_0} - 16)} \sum_{i < j} [e^{-\alpha(r_{ij} - r_0)} (e^{-\alpha(r_{ij} - r_0)} - 2)] \right. \\
& \left. - \frac{1}{2} \sum_{i=1}^N (x_i^2 + \frac{\omega_y^2}{\omega_x^2} y_i^2 + \frac{\omega_z^2}{\omega_x^2} z_i^2) \right] \psi(\vec{r}) \\
= & \quad -E_0 \psi(\vec{r}) \tag{31}
\end{aligned}$$

With $\omega_x = \omega_y = \frac{\omega_z}{\sqrt{\lambda}}$, the above eqn becomes,

$$\begin{aligned}
& \left[\frac{1}{2} \sum_{i=1}^N \nabla_i^2 - 4 \frac{a\alpha^3}{se^{\alpha r_0} (e^{\alpha r_0} - 16)} \sum_{i < j} [e^{-\alpha(r_{ij} - r_0)} (e^{-\alpha(r_{ij} - r_0)} - 2)] \right. \\
& \left. - \frac{1}{2} \sum_{i=1}^N [x_i^2 + y_i^2 + \lambda z_i^2] \right] \psi(\vec{r}) \\
= & \quad -E_0 \psi(\vec{r}) \tag{32}
\end{aligned}$$

$$\begin{aligned}
& \left[\frac{1}{2} \sum_{i=1}^N \nabla_i^2 - \gamma \sum_{i < j} [e^{-\alpha(r_{ij} - r_0)} (e^{-\alpha(r_{ij} - r_0)} - 2)] \right. \\
& \left. - \frac{1}{2} \sum_{i=1}^N [x_i^2 + y_i^2 + \lambda z_i^2] \right] \psi(\vec{r}) \\
= & \quad -E_0 \psi(\vec{r}) \tag{33}
\end{aligned}$$

Now for $\alpha = .35$ and $r_0 = 11.65$ (both in oscillator units)[20]. We have checked that for these choice of parameters, Morse solution is extremely

good. $a = 52 \times 10^{-10}$, $s = .12 \times 10^{-5}$, the interaction strength γ is given by

$$\gamma = 4 \frac{a\alpha^3}{se^{\alpha r_0}(e^{\alpha r_0} - 16)} = 2.92 \times 10^{-7} \quad (34)$$

For mean field calculation the value of interaction strength was taken to be 4.33×10^{-3} . For this problem we are interested in the limit $\gamma \ll 1$. The case $\gamma \gg 1$ is usually known as the Thomas Fermi limit. For $\gamma = 2.92 \times 10^{-7}$, the eigenvalue equation reduces to a minimally perturbed system of d dimensional anisotropic oscillator where $d = 3N$ and N is the number of particles. The whole concept of bound states of Morse dimers is very outside the range of this limit, so the nonexistence of two-body bound states is ensured by choosing the above parameters.

Even though $\gamma \ll 1$, we solve the eigenvalue eqn nonperturbatively with Generalized Feynman-Kac procedure. Energies and frequencies at zero temperature are obtained by solving Eq. (4) and using Eq.(7). To calculate the analogous quantities at finite temperature we use Eq.(16). We can get the energy of the condensate from Eq.(7) and Eq.(16) by generating a large number of paths and then averaging the results for each path. Since original Feynman-Kac method [12] is computationally inefficient we incorporate importance sampling in our random walk and use trial function of the form given in Eq.(20)

Evaluation of temperature dependent mode frequencies

: Following the prescription in [4], we see that for a fixed 'N' the above relationship generates the condensation fraction N_0/N as a function of time. One can generate this from the experiment also. From the thermodynamical limit we get N_0 as a function of time and run our zero temperature code with same number of this N_0 as the dynamics of the finite temperature condensate are essentially the same as those of a zero temperature condensate with the same value of N_0 . Later in Fig. 8 (our data) of Section 4.2, we see the effects of interaction on the condensation fraction.

4 Results

4.1 Condensate Excitation spectra at T=0 for different symmetries

We chose Rb^{87} as an example of a weakly interacting dilute Bose gas as in Ref[2]. We simulate 100 Rb atoms interacting with Morse potential. We choose $a = 52 \times 10^{-10}$, length scale s of the problem as $.12 \times 10^{-5}$. In the following table, we show the ground state energy of the particle. With repulsive interactions, the Energy/particle increases with the increase in number of particles in the trap [Fig 2-5] whereas the energy gap between the different symmetry states decreases as evident from Fig.6 and 7.

Table 1: **Results for the ground state energy of Rb^{87} atoms in a trap with $\omega_x = \omega_y = 1, \lambda = \omega_z = \sqrt{8}$ in the interacting case ; The table shows how energy varies with the number of particles in the Gross Pitaevski(GP) case [21] and GFK method.**

N	E/N(GP)	E/N(GFK)
1	2.414	2.414 213
10		2.4154816(3)
40		2.419708(1)
70		2.42401(1)
100	2.66	2.42815(1)
200	3.21	

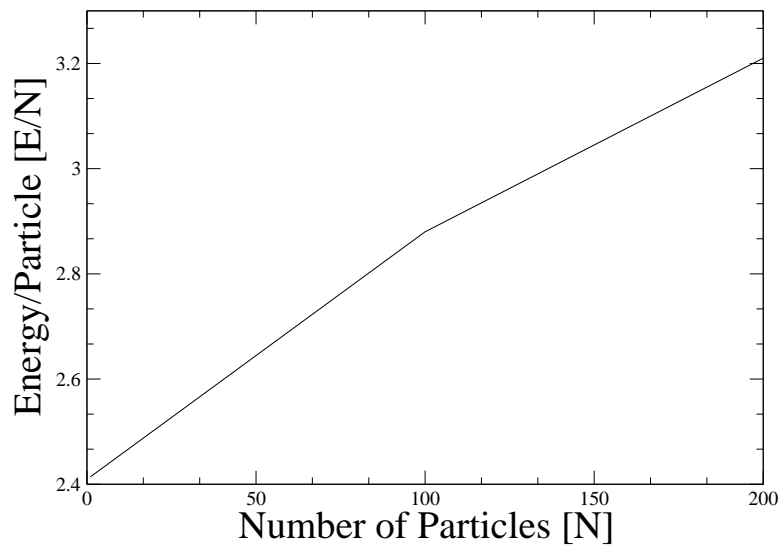


Figure 1: A plot for the Condensate Energy/Particle versus Number of atoms in the trap for 200 particles for the ground state from data in the literature[21]

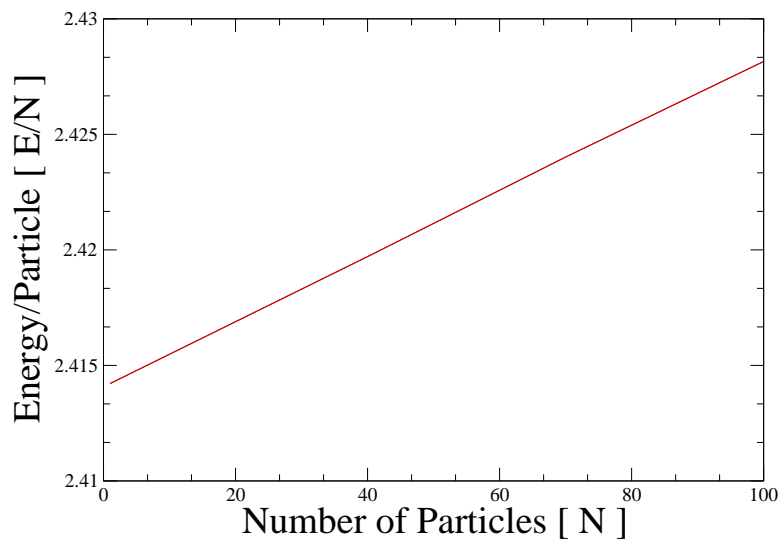


Figure 2: A plot for the Condensate Energy/Particle versus Number of atoms in trap for 100 particles for the ground state for the ground state: $n_z = n_\rho = m = 0$; this work

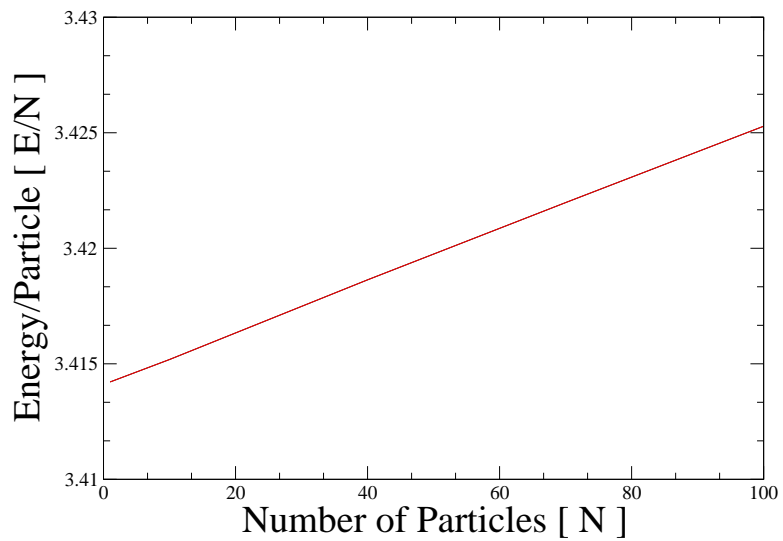


Figure 3: A plot for the Condensate Energy/Particle versus Number of atoms in trap for 100 particles for the 1st excited state : $n_z = n_\rho = 0, m = 1$; this work

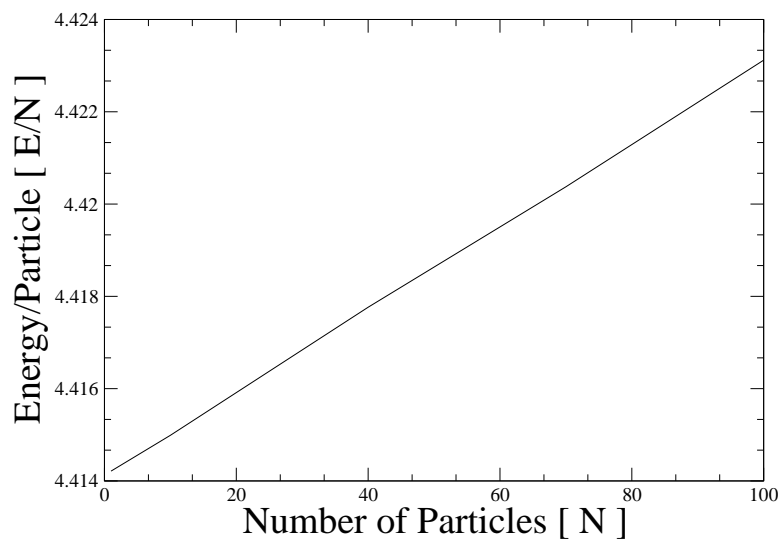


Figure 4: A plot for the Condensate Energy/Particle versus Number of atoms in trap for 100 particles for the 2nd excited state: $n_z = n_\rho = 0, m = 2$; this work

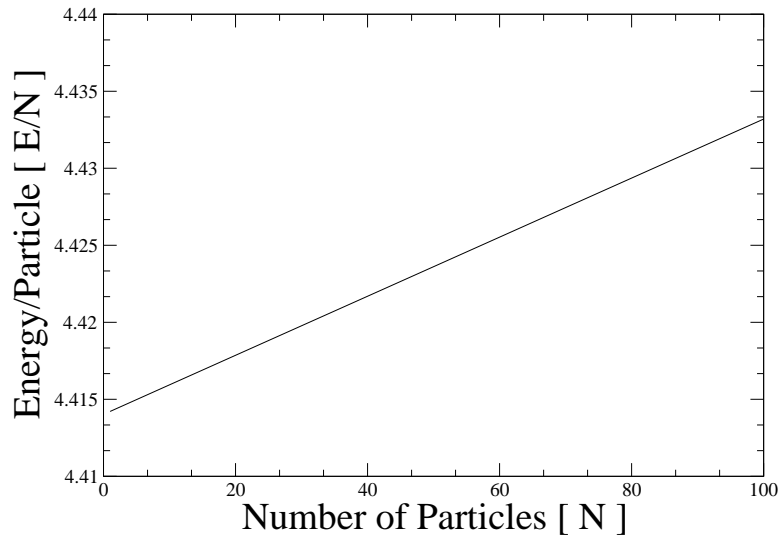


Figure 5: A plot for the Condensate Energy/Particle versus Number of atoms in trap for 100 particles for the 3rd excited state: $n_z = m = 0, n_\rho = 1$; this work

Table 2: **frequency ω for lowest lying modes**

N	quantum numbers	ω
100	$n_z = 0 = n_\rho = m = 0$	0
100	$n_z = 0 = n_\rho, m = 1$	0.997128
100	$n_z = 0 = n_\rho, m = 2$	1.994966

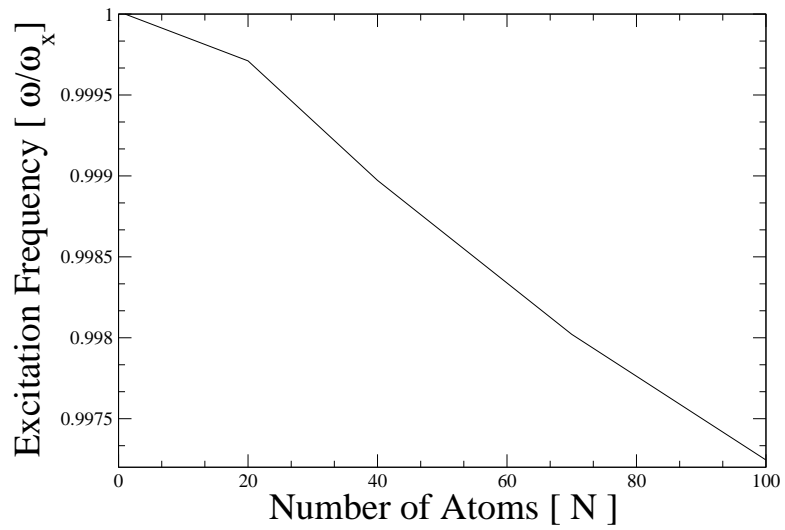


Figure 6: A plot of Excitation Frequency vs Number of Atoms for lowest lying $m=1$;this work

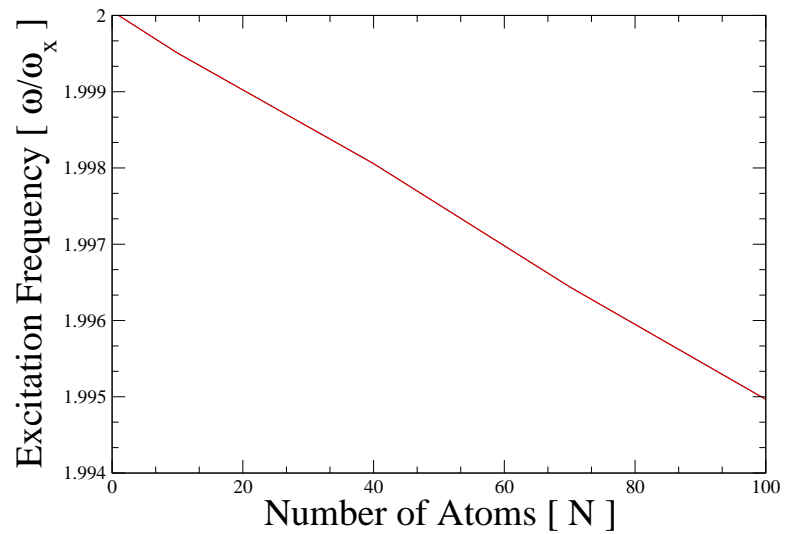


Figure 7: A plot of Excitation Frequency vs Number of Atoms for lowest lying $m=2$;this work

4.2 Effects of temperature on condensation fraction

Density of condensate atoms decreases in the trap as temperature increases. This lowers the interaction energy of the condensate atoms resulting in a shift in the critical temperature.

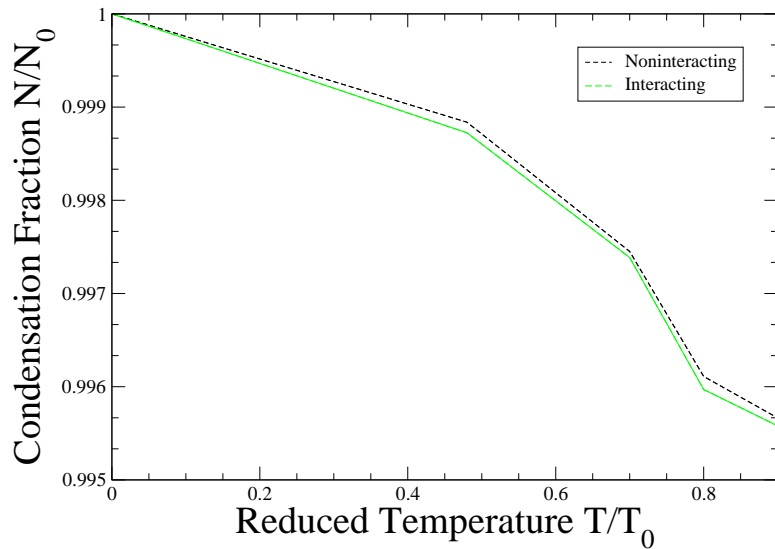


Figure 8: Condensation fraction vs Reduced Temperature ; this work. The inner curve corresponds to the 100 interacting atoms and the outer one corresponds to the noninteracting case. The number of condensed particles decreases with the interaction

4.3 Effects of temperature on the frequency shifts; comparison with other experiments and theories

Underneath from JILA data, one observes a large temperature dependent frequency shift for both $m=0$ and $m=2$ modes. For $m=2$ mode, starting from Stringari limit it decreases all the way up to $0.9T_c$ whereas for $m=0$ mode it shows a rising trend with rise in temperature. In Fig.12 [Ref 4] one observes that theoretical data agrees with JILA top only up to $0.6T_c$ whereas our data [Fig. 10] agrees with JILA TOP data and theoretical data in Fig. 11 Ref [5] all the way to $0.9T_c$. Temperature variation of $m=0$ mode from our data agrees with MIT[22] and Ref[5] but differs from JILA data.

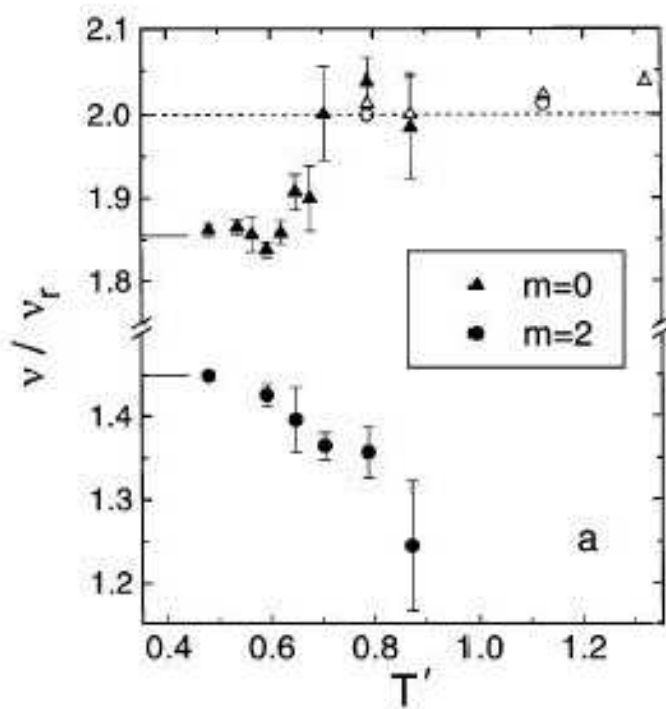


Figure 9: Effects of temperature on $m=2$ mode; JILA data; The data marked by triangles represent the $m=0$ mode and solid circles represent $m=2$ mode

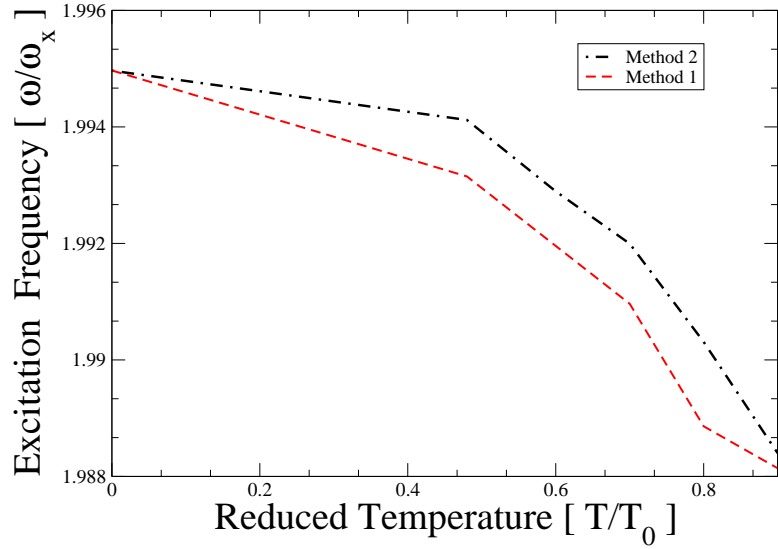


Figure 10: Effects of temperature on $m=2$ mode; this work. The top curve from equivalent $T=0$ system[method 2], the bottom curve by putting temperature directly[method 1]. Both show agreement with experimental data all the way up to $0.9T_c$

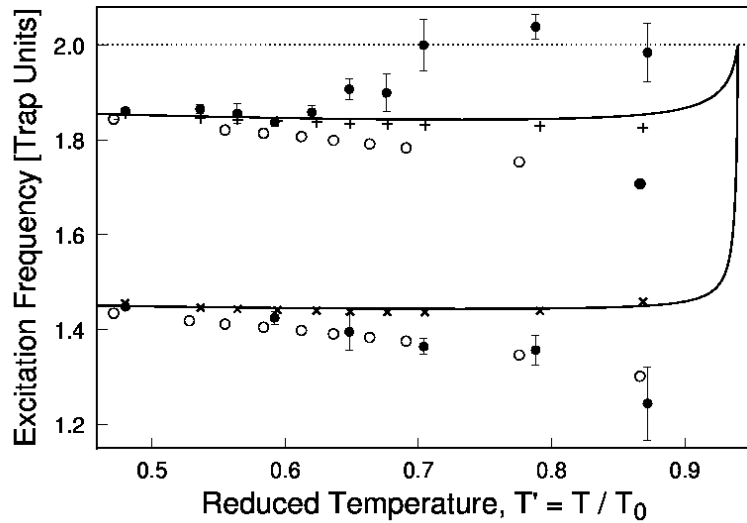


Figure 11: Effects of temperature on $m=2$ mode; Ref 5 which agrees with JILA for $m=2$ mode but shows opposite trend for $m=0$ mode

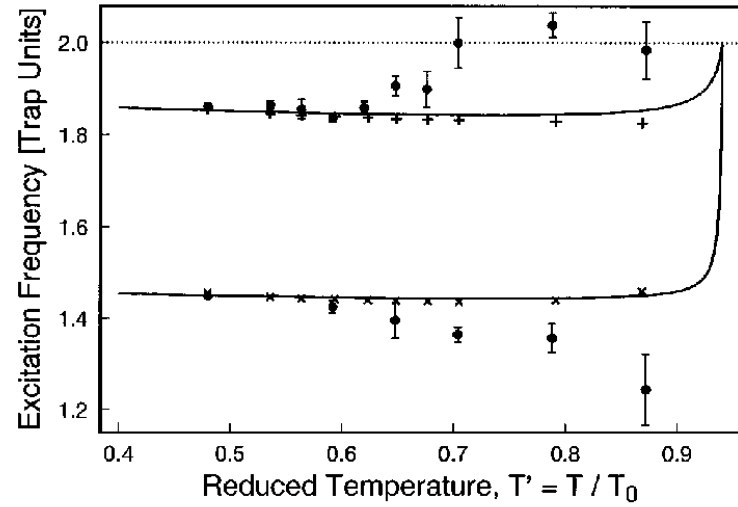


Figure 12: Effects of temperature on $m=2$ and $m=0$ mode; Edwards data. It shows a similar trend with JILA experiment for $m=0$ mode, but disagrees for $m=2$ mode near critical temperature

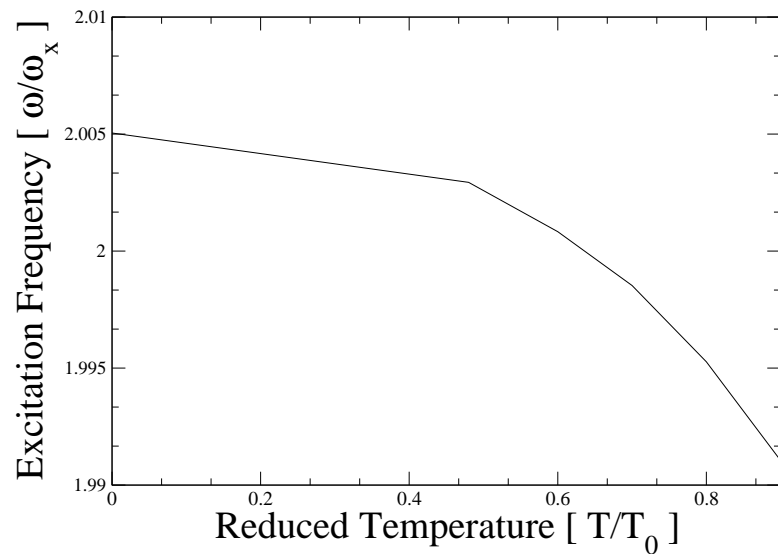


Figure 13: Effects of temperature on $m=0$ mode from equivalent $T=0$ system[this work], shows resemblance with MIT and Ref 5

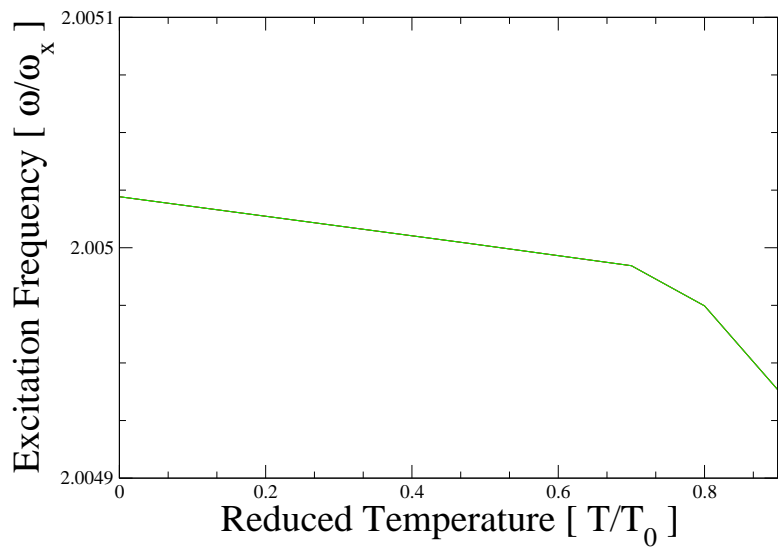


Figure 14: Effects of temperature on $m=0$ mode from GFK by putting temperature directly[this work], also shows resemblance with MIT and Ref 5

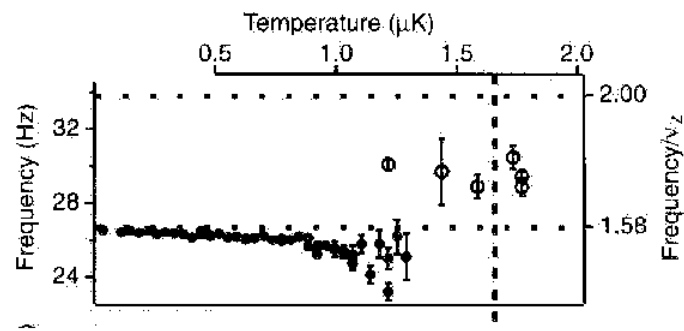


Figure 15: Effects of temperature on $m=0$ mode; MIT data, shows opposite trend with that of JILA

5 Conclusions:

Comparing our data with JILA we see that for $m = 2$ mode, excitation frequencies decrease as temperatures go up. Since we are dealing with only 100 Rb atoms, our zero temperature limit is different from Stringari limit. We could not compare datas on the same graph because of the difference in the number of particles. Almost all other theoretical work show a reverse trend - frequencies increase with rise in temperature. At $T=0$, as N increases the energies grow, but the splitting between the ground and excited state decreases - an essential feature of Bose Condensation. This tells us how successful we have been in bringing out the many body effect in our model. From our simulations for $m=2$, the frequencies decrease with rise in temperature. The other theoretical work shows the reverse trend [4] [ref to Fig. 12]. Our work [Fig. 10] agrees with JILA experiment ($m=2$ mode).

We have used GFK to bring out the many body effects between the cold Rb atoms. Numerical work with bare Feynman-Kac procedure employing modern computers was reported[11] for the first time for few electron systems after forty years of original work[12] and seemed to be real useful for calculating atomic ground states[23]. Tremendous success in atomic physics motivated us to apply it to condensed matter physics[24].

We have been successful in achieving a lower value for Rb ground state than that obtained by Gross-Pitaevski technique[21]. Blume et al [25] obtained results in the isotropic case, which was higher than the variational calculations. For the first time we have calculated finite temperature properties beyond mean field approximation by Quantum Monte Carlo technique. We have calculated spectrum of Rb gas by considering realistic potentials like Morse potential etc. instead of conventional pseudopotentials for the first time. We have found an alternative to Gross-Pitaevski technique and other mean field calculations.

We found that considering the dynamics of condensates alone and the effect of finite temperature as static thermal cloud, we do not achieve the upward shifts of frequencies as shown by JILA data for $m=0$ mode[Fig. 9]. Our results rather agree more with the work done by MIT group[22].

As a matter of fact, we agree with Ref [5] that as $m=0$ happens to be a coupled mode, we need to consider the dynamics of thermal cloud to obtain a satisfactory agreement with the experimental data. The reason that the quantitative agreement between the Stringari limit predicted by us for $m=0$ mode and the experiments is not good, might be the use of Gaussian wave functions as the trial functions. It is legitimate to use it for $m=2$ mode as JILA experiment has not been done in the Thomas Fermi limit. But for $m=0$ mode we need to include correlations in the wave function as $m=0$ is a coupled mode. This would be a nontrivial extension of the present work and will be reported elsewhere.

We are dealing with only 100 atoms. Nonetheless we have been able to demonstrate some of the 'Holy Grails' of Bose Condensation, lowering of the gap between vortex and ground states with the increase in number of atoms and lowering of condensation fraction in the case of interacting case. In our non mean field study, we see agreement with experimental study all the way to $T = 0.9T_c$ [Fig. 10]. The method is extremely easy to implement and our fortran code at this point consists of about 270 lines. We employ an algorithm which is essentially parallel in nature so that eventually we can parallelize our code and calculate thermodynamic properties of bigger systems (of the order of 2000 atoms) taking advantage of new computer architectures. This work is in progress. We are continuing on this problem and hope that this technique will inspire others to do similar calculations.

References

- [1] M. H. Anderson, J.R. Ensher, M.R. Matthews, C. E. Wieman E. A. Cornell, *Science* **269**,198 (1995)
- [2] D. S. Jin, M. R. Mathews, J. R. Ensher, C. E. Wieman and E. A. Cornell *Phys Rev Lett* **78** 764 (1997)
- [3] D. A. Hutchinson, E. Zeremba and A. Griffin, *Phys Rev Lett.*, **78** (1997).
- [4] R.J. Dodd, M. Edwards, C. W. Clark and K. Burnett **57** , *Phys Rev A*,**57** , R32 (1998).
- [5] D. A. Hutchinson, R. J. Dodd and K. Burnett, *Phys. Rev. Lett* **81**, 2198 (1998)
- [6] H. Shi and W. Zheng, *Phys. Rev A* **59**, 1562 (1999)
- [7] V. L. Ginzburg and L.P. Pitaevski, *Zh. Eksp. Teor. Fiz.*, **34** 1240(1958)[*Sov. Phys. JETP* 7, 858 (1958)], E.P. Gross, *J. Math Phys.***4**, 195(1963)
- [8] V. N. Popov, *Functional Integrals and Collective modes* (Cambridge University Press, New York, 1987),Ch.6.
- [9] dissertation submitted to JILA.
- [10] M. Cafferel and P. Claverie, *J. Chem Phys.* **88** , 1088 (1988), **88**, 1100 (1988)
- [11] A. Korzeniowski, J. L. Fry, D.E. Orr and N. G. Fazleev, *Phys. Rev. Lett.* **69**, 893,(1992)
- [12] M. D. Donsker and M. Kac, *J. Res. Natl. Bur. Stand.*, **44** 581 (1950), see also, M. Kac in *Proceedings of the Second Berkley Symposium* (Berkley Press, California, 1951)
- [13] M. D. Donsker and S. R. Varadhan, in *Proc. of the International Conference on Function space Integration* (Oxford Univ. Press 1975)pp. 15-33.

- [14] Feynman And Hibbs, Quantum Mechanics and Path Integrals, (McGraw-Hill, NY,1965).
- [15] Y. A. Kagan, E. L. Surkov, and G. V. Shlyapnikov, Phys. Rev A **55** R18 (1997).
- [16] R. J. Dodd, J Res. Natl Inst. Stand. Technol **101**,545(1996)
- [17] W. Ketterle, D. S. Durpee and D. M. Stamper-Kurn in the Proceedings of international School of Physics edited by M. Inguscio, S. Stringari, C. E. Wieman (1998)
- [18] J. L DuBois, Ph D dissertation, University of Delaware,(2003).
- [19] W. Krauth, Phys. Rev Lett, **77** 3695(1996)
- [20] B. D. Esry, Phys. Rev A **55**, 1147 1997,
- [21] F. Dalfovo and S. Stringari, Phys. Rev A **53**, 2477(1996).
- [22] D. M Stampur-Kurn, H. J. Miesner, S. Inouye, M. R. Andrews, and W. Ketterle, Phys. Rev. Lett. **81**, 500 (1998)
- [23] J. Madox, Nature **358** 707 (1992)
- [24] S. Datta, J. L Fry, N. G. Fazleev, S. A. Alexander and R. L. Coldwell, Phys Rev A **61** (2000) R030502, Ph. D dissertation, The University of Texas at Arlington,(1996).
- [25] D. Blume, C. H. Green, Phys. Rev A **63** 063601(2001)

Acknowledgements:

Financial help from DST (under Young Scientist Scheme (award no. SR/FTP/-76/2001)) is gratefully acknowledged. The author would like to thank Prof J. K . Bhattacharjee, Indian Association for the Cultivation of Science, India for suggesting the problem and many stimulating discussions and also Prof C. W. Clark of NIST,USA for suggesting some useful references and Prof P. Nightingale of Univ of Rhode Island, USA for many useful discussions on the bound state of Rb.